Quaternary Research 75 (2011) 624–635

Contents lists available at ScienceDirect

Quaternary Research

journal homepage: www.elsevier.com/locate/yqres

Late Quaternary cryptotephra detection and correlation in loess in northeastern Japan using cummingtonite geochemistry

Tabito Matsu'ura [a,b,*], Isoji Miyagi [a], Akira Furusawa [c]

[a] Geological Survey of Japan, AIST, Site 7, 1-1-1 Higashi, Tsukuba, Ibaraki 305-8567, Japan
[b] Now at Japan Nuclear Energy Safety Organization (JNES), Kamiya-cho MT Bldg., 4-3-20, Toranomon, Minato-ku, Tokyo, 105-0001, Japan
[c] Furusawa Geological Survey, 93-7 Yashiki, Tosaki-cho, Okazaki, Aichi 444-0840, Japan

ARTICLE INFO

Article history:
Received 10 December 2009
Available online 14 January 2011

Keywords:
Late Quaternary
Cryptotephra
Tephra
Cummingtonite
Correlation tool
Chemical analysis
Loess deposits
Northeastern Japan

ABSTRACT

We detected late Pleistocene cummingtonite-bearing cryptotephras in loess deposits in NE Japan and correlated them with known tephras elsewhere by using major-element compositions of the cummingtonite. This is the first time cryptotephras have been identified by analysis of a crystal phase rather than glass shards. In central NE Japan, four cummingtonite-bearing tephras, the Ichihasama pumice, the Dokusawa tephra, the Naruko–Nisaka tephra, and the Adachi–Medeshima tephra, are present in late Pleistocene loess deposits. Because the cummingtonite chemistry of each tephra is different and characteristic, it is potentially a powerful tool for detecting and identifying cryptotephras. An unidentified cummingtonite-bearing cryptotephra previously reported to be present in the late Pleistocene loess deposits at Kesennuma (Pacific coast) did not correlate with any of the known cummingtonite-bearing tephras in central NE Japan, but instead with the Numazawa–Kanayama tephra (erupted from the Numazawa caldera, southern NE Japan), although Kesennuma is well beyond the previously reported area of the distribution of the Numazawa–Kanayama tephra. Three new cummingtonite-bearing cryptotephras in the mid and late Pleistocene loess deposits (estimated to be less than 82 ka, 100–200 ka, and ca. 250 ka) on the Isawa upland were also detected.

Introduction

Cummingtonite, a pale-colored mineral of the amphibole group with the formula $(Mg,Fe)_7Si_8O_{22}(OH)_2$, is sometimes reported in Quaternary tephras in and around Japan (Machida and Arai, 2003). Only 10 of 340 late Pleistocene tephras (about 3%) are cummingtonite-bearing (Fig. 1; Machida and Arai, 2003). Thus, cummingtonite is distinctive in late Pleistocene tephrostratigraphy, and cryptotephras, which are essentially invisible to the naked eye (Lowe and Hunt, 2001), can be identified and correlated if they contain it.

At many distal sites, glass shards or mineral grains (crystals) derived from tephra falls are often difficult to detect. Nevertheless, there has been some success in detecting cryptotephras in peat (Gehrels et al., 2006, 2008; Payne et al., 2008), lacustrine sediments (de Fontaine et al., 2007; Wagner et al., 2008), marine sediments (Lowe et al., 2007; Lim et al., 2008; and Wulf et al., 2008), and ice cores (Lowe, 2008; Wastegård and Davies, 2009; and Davies et al., 2010) primarily as concentrations of volcanic glass shards. Well-preserved glass shards in these sediments can be dated by applying radiometric methods, including ^{14}C dating, to encasing sediments, by ice-core annual-accumulation modeling, or by correlation with marine oxygen isotope stages (MISs: Bassinot et al., 1994). However, glass shards may also be dissolved during weathering, and in terrestrial sediments such as loess deposits they therefore may not be evident.

Although the temporal resolution of loess deposits is generally poor because their sedimentation rates are lower than those of peat or lacustrine and marine sediments, loess deposits that contain tephras or cryptotephras are useful both for estimating long-term volcanic hazards and for providing the chronology of extensive mid to late Quaternary terrestrial sequences. In this paper, we focus on tephra-derived particles composed of cummingtonite, which are less likely than glass shards to be dissolved by weathering. The cummingtonite concentrations in sediments are potentially distinctive cryptotephra-based marker horizons, especially useful because few late Pleistocene tephras in Japan are cummingtonite-bearing.

Concentrations of cummingtonite grains in the loess deposits on the MIS 5.5 marine terrace surface in the central part of northeastern (NE) Japan (Matsu'ura et al., 2009) have been divided into two groups by optical analysis. One group correlates with the Dokusawa tephra (Dks: Matsu'ura et al., 2002), but the other is of indeterminate origin. The second group may be a hitherto-unreported cummingtonite-bearing tephra, or it may represent a previously named tephra not previously detected in this part of Japan.

The optical characteristics of cummingtonite are not critically different from those of hornblende. Therefore, in this study, we used calcium chemistry data to differentiate cummingtonite from hornblende.

* Corresponding author. Fax: +81 3 4511 1598.
E-mail address: matsuura-tabito@jnes.go.jp (T. Matsu'ura).

0033-5894/$ – see front matter © 2010 University of Washington. Published by Elsevier Inc. All rights reserved.
doi:10.1016/j.yqres.2010.12.004

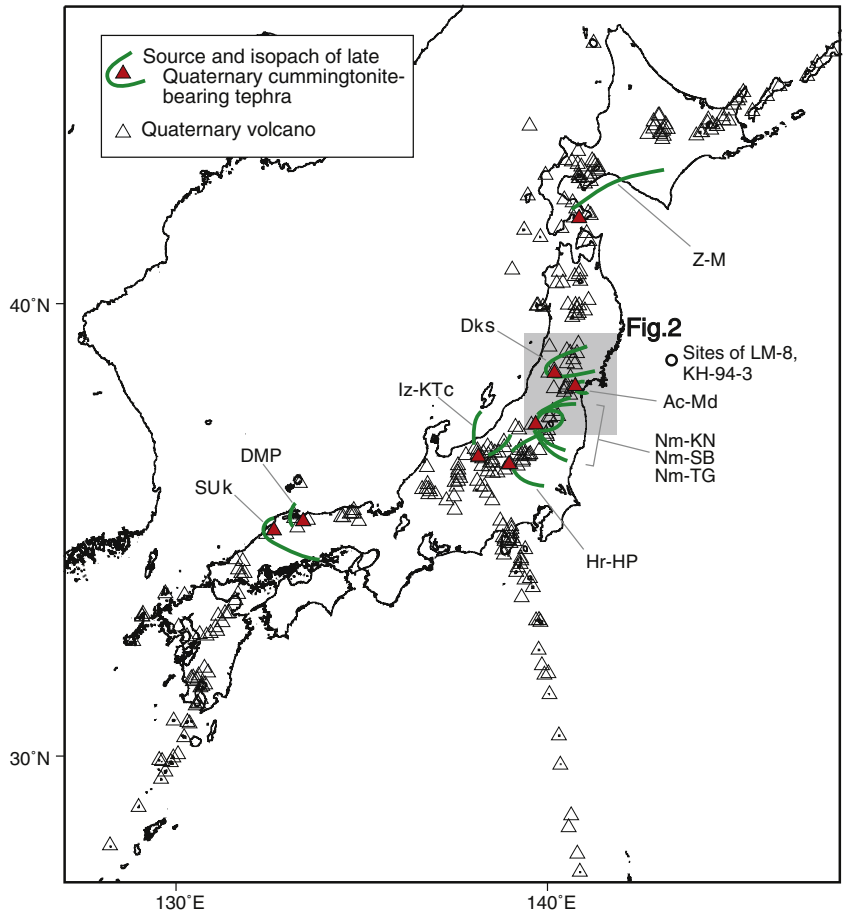

Figure 1. Map showing the distributions of late Quaternary cummingtonite-bearing tephras in and around Japan. Sources of tephra isopach information and tephra abbreviations: SUk (Sambe–Ukinuno), DMP (Daisen–Matsue), Hr–HP (Haruna–Hassaki), Ac–Md (Adachi–Medeshima), and Z–M (Zenikame–Menagawa), Machida and Arai (2003); Iz–KTc (Iizuna–Kamitaru c), Suzuki (2001); Nm–KN (Numazawa–Kanayama), Suzuki and Soda (1994); Nm–SB (Numazawa–Shibahara) and Nm–TG (Numazawa–Tagashira), Suzuki et al. (2004); Dks (Dokusawa), Matsu'ura et al. (2002).

Although geochemical analyses of minerals (including cummingtonite) have been used before to correlate tephras (e.g., Smith and Leeman, 1982; Lowe, 1988; Shane et al., 1998, 2003; Matsu'ura et al., 2003; and Suzuki, 2008), cummingtonite chemistry has not been used previously to characterize, and hence distinguish, cummingtonite-bearing cryptotephras.

Late Quaternary cummingtonite-bearing tephras are distributed in North America (e.g., Mullineaux, 1986; Geschwind and Rutherford, 1992) and New Zealand (e.g., Smith et al., 2005, 2006; Lowe et al., 2008) as well as in Japan (Machida and Arai, 2003). Thus, our novel technique to characterize and distinguish cummingtonite-bearing cryptotephras has wide applicability for establishing tephrostratigraphy using cryptotephras. Well-dated chronostratigraphies developed using cummingtonite-bearing cryptotephras should be useful in establishing chronological relationships among sediments and landforms.

We first analyzed the major-element compositions of cummingtonite from named tephras in NE Japan. We then investigated the vertical variation in cummingtonite chemistry in the late Pleistocene loess deposits in the vicinity of Kesennuma, central NE Japan, which is downwind of the source volcanoes, to detect cummingtonite-bearing cryptotephras. Finally, we constructed the cummingtonite-bearing cryptotephra stratigraphy of the loess deposits and correlated the cryptotephras with the reported tephras on the basis of their cummingtonite major-element chemistry. We show that cummingtonite-bearing cryptotephras can be useful for enhancing mid Pleistocene tephrostratigraphy in NE Japan and for developing the chronology of terrace deposits in the same region.

Materials and methods

We sampled named tephras distributed in the Kesennuma area, as shown by isopach maps at localities 2–8 (Fig. 2), to identify and characterize cummingtonite-bearing tephras. Then we obtained samples of the loess deposits (including cryptotephras) on terraces by rotary coring in the vicinity of Kesennuma (loc. 1), on the Pacific coast of Japan (Fig. 2). For cryptotephra identification, we also sampled cummingtonite-bearing tephras distributed in NE Japan but not found at Kesennuma. Core samples and samples from outcrops were sieved under running water through disposable 0.125-mm and 0.0625-mm sieves. The disposable sieves were changed between samples to prevent contamination. The residues were dried, embedded in resin, and mounted on slides for examination of the grain composition. For the chemical analyses, about ten cummingtonite grains were picked from each sample, mounted in resin, and polished flat.

The major-element chemical composition of the cummingtonite grains was analyzed by scanning electron microscope with energy-dispersive spectrometry (SEM/EDS: Horiba Emax Energy EX-250). Major elements were measured with a counting time of 150 s. An accelerating voltage of 15 kV and a beam current of 0.3 nA with beam

https://doi.org/10.1016/j.yqres.2010.12.004 Published online by Cambridge University Press

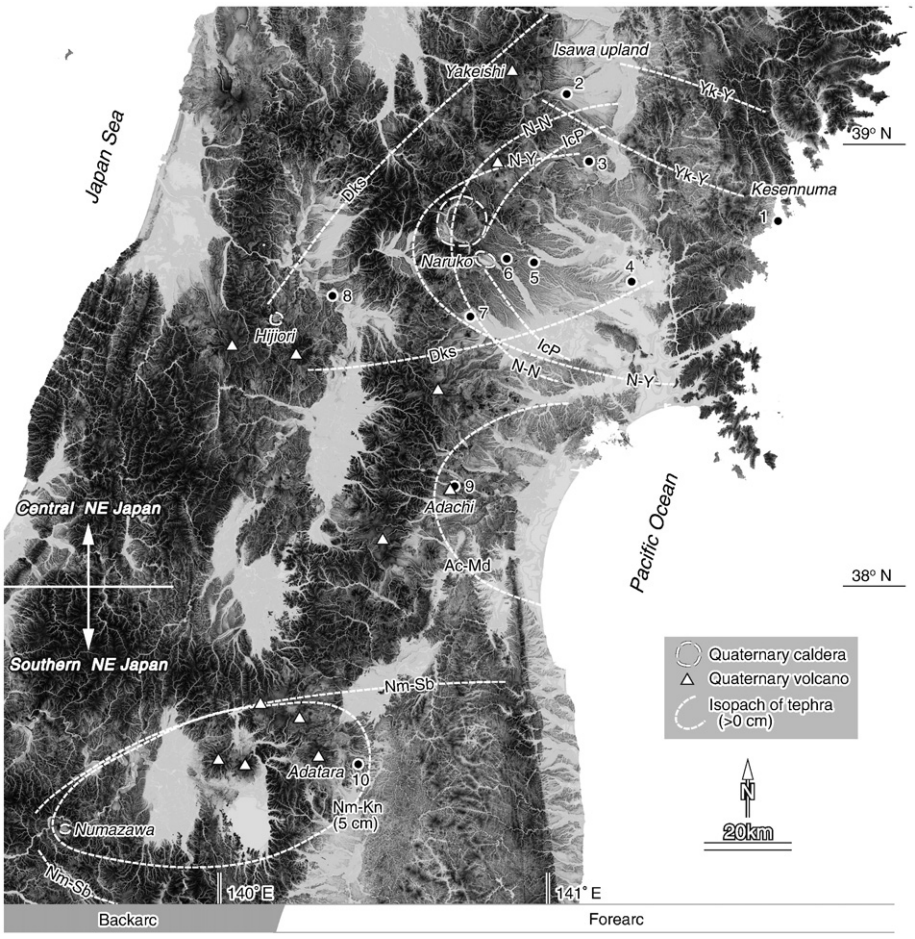

Figure 2. Map showing the distributions of cummingtonite-bearing tephras and locations of survey points in central NE Japan. The distributions of cummingtonite-free tephras in the Kesennuma area are also shown. Isopachs are the 0-cm isopach, except the 5-cm isopach of the Nm–KN tephra is shown.

diameter of 150 nm were used for scanning a 4-μm grid of the targeted cummingtonite grain. The ZAF procedure was applied to correct for atomic number and fluorescence effects. We use Fe–Mg plots to distinguish cummingtonite of different chemical compositions and report our results as the numbers of Fe and Mg cations per unit cell (on the basis of O = 23).

Late Pleistocene tephras in central and southern NE Japan

Numerous Quaternary volcanoes are distributed in the backarc region of NE Japan (Fig. 2). Here, we refer to the areas north and south of 38ºN (Fig. 2) as central and southern NE Japan, respectively. Some volcanoes (calderas) that erupted during the late Pleistocene provided cummingtonite-bearing tephras to the forearc: namely, the Dokusawa tephra (Dks), from the Hijiori volcano or another volcano in its vicinity, MIS 5.2–5.3 (Matsu'ura et al., 2002); the Naruko–Nisaka tephra (N–N), from the Naruko caldera, MIS 5.2–5.3 (Soda, 1989; Matsu'ura et al., 2009); the Adachi–Medeshima tephra (Ac–Md), from the Adachi volcano, older than MIS 5.2 (Yagi and Soda, 1989); the Numazawa–Shibahara tephra (Nm–SB) from the Numazawa caldera, 110 ka or MIS 5.4–5.3 (Suzuki et al., 2004); and the Numazawa–Kanayama tephra (Nm–KN) from the Numazawa caldera, 50–55 ka (Suzuki and Soda, 1994). No cummingtonite-bearing tephras were observed stratigraphically above the Aso-4 tephra (MIS 5.2) in marine cores KH-94-3 and LM-8, obtained offshore of Kesennuma (Aoki and Arai, 2000; Aoki, 2008; Fig. 1). Dks, N–N, and the Naruko–Yanagisawa tephra (N–Y: a cummingtonite-free tephra erupted from the Naruko volcano) were previously detected in loess deposits at loc. 1 (Kesennuma: Fig. 2) as cryptotephras on the basis of glass-shard geochemistry (Matsu'ura et al., 2009). Matsu'ura et al. (2009) also detected small quantities of cummingtonite grains in the loess deposits. They divided these grains into two groups on the basis of their refractive indices: one (n_2, 1.662–1.666) could be correlated with Dks or N–N, but the other (n_2, 1.657–1.662) represented an unknown cummingtonite-bearing cryptotephra with unknown source, eruptive age, and distribution (Matsu'ura et al., 2009).

Cummingtonite-bearing tephras potentially at Kesennuma as indicated by previous isopach mapping

Ichihasama tephra (IcP)

The Ichihasama tephra (IcP) (Soda, 1989) may have erupted from the Naruko volcano or another volcano in its vicinity in central NE Japan (Machida and Arai, 2003). The eruptive age of IcP is greater than MIS 5.4 because it is stratigraphically below the Toya tephra (Toya, MIS 5.4: Soda, 1989; Machida and Arai, 2003). IcP is below Dks at loc. 4 and consists of fallout pumice and ash (Fig. 3). Its reported heavy mineral assemblage consists of orthopyroxene and magnetite (Soda, 1989), but we detected minor amounts of cummingtonite in IcP by careful microscopic examination. We determined the Fe and Mg contents of the cummingtonite by SEM/EDS (sample 4I1) to be 2.55–3.87 and 3.27–4.77 cations per unit cell, respectively (Fig. 4a).

https://doi.org/10.1016/j.yqres.2010.12.004 Published online by Cambridge University Press

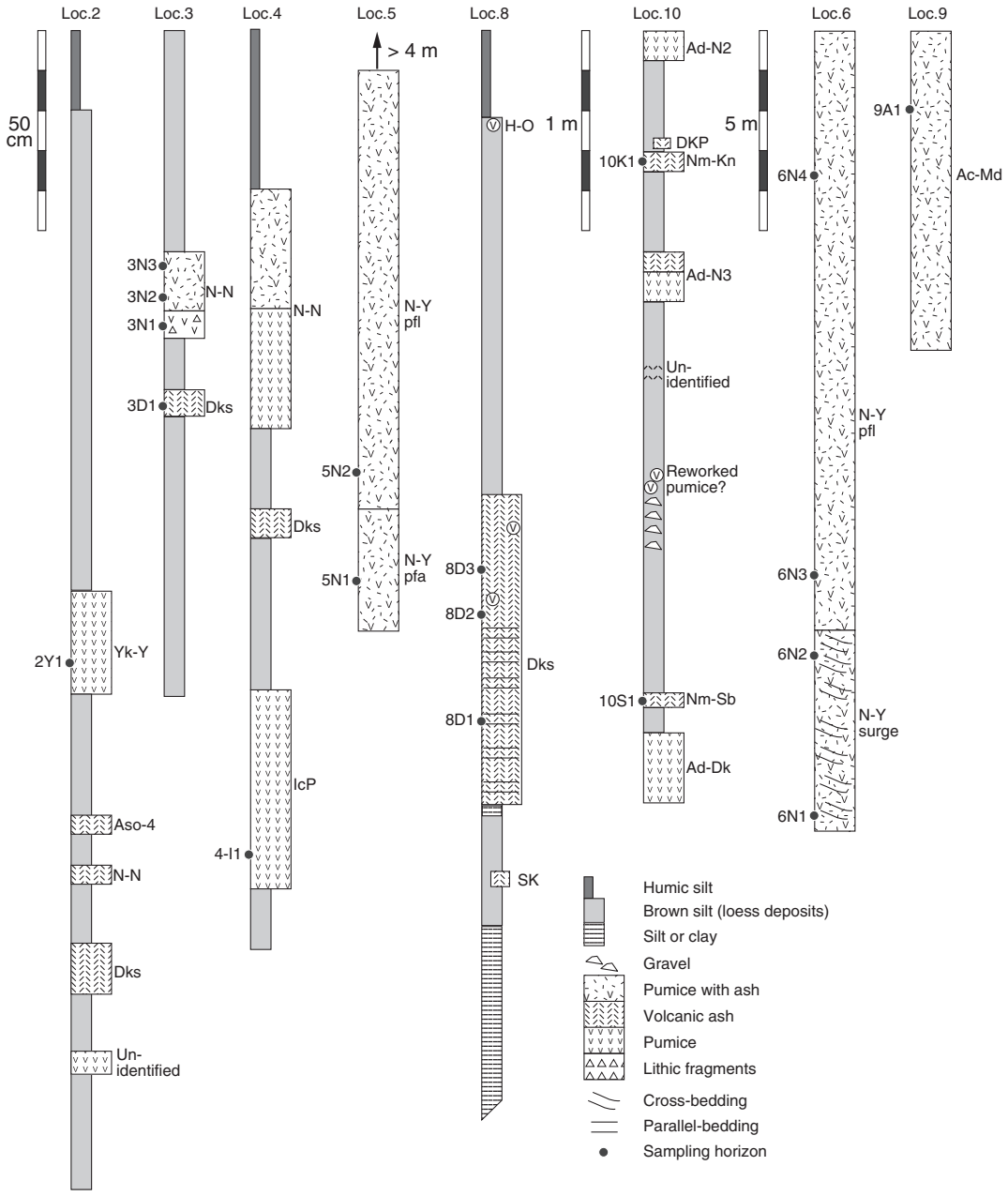

Figure 3. Geological columns of outcrops. Locations are shown in Figure 2. Tephra abbreviations and eruptive ages: H–O, Hijiori–Obanazawa (12 cal ka BP); N–Y, Naruko–Yanagisawa (50.9 ^{14}C yr BP; thermoluminescence dates, 31.6–57.0 ka; FT dates, 40.3–63.4 ka); Nm–KN, Numazawa–Kanayama (ca. 60 ka); Yk–Y, Yakeishi–Yamagata (FT date, 82 ± 19 ka); Aso-4 (MIS 5.2, 86.8–87.3 ka, Aoki, 2008); N–N, Naruko–Nisaka (MIS 5.2–5.3); Dks, Dokusawa (MIS 5.2–5.3); SK, Sambe–Kisuki (MIS 5.3); IcP, Ichihasama (older than MIS 5.4); Ac–Md, Adachi–Medeshima (older than MIS 5.2); Nm–SB, Numazawa–Shibahara (MIS 5.5). See text for eruptive ages of tephras. Abbreviations: pfl and pfa are pyroclastic flow and pyroclastic fall deposits, respectively.

Dokusawa tephra (Dks)

The Dokusawa tephra (Dks) was erupted from the backarc region in central NE Japan from the Hijiori caldera or another volcano in its vicinity (Matsu'ura et al., 2002; Fig. 2). The eruptive age of Dks is MIS 5.2–5.3, because it is stratigraphically above the Ontake–Pm1 tephra (On–Pm1, MIS 5.3), and it is below the Aso-4 tephra (MIS 5.2) (Matsu'ura et al., 2002, 2003; Aoki, 2008). At sites sampled in this study, Dks is above the Sambe–Kisuki tephra (SK, MIS 5.3) at loc. 8 and IcP at loc. 4, and it is below N–N at locs. 2, 3, and 4, Aso-4 at loc. 2, and the Hijiori–Obanazawa tephra (H–O, ca. 12,000 cal yr BP; Miyagi, 2004) at loc. 8 (Fig. 3). At these locations, Dks consists of fallout ash, and at loc. 8 it includes a minor amount of pumice (Fig. 3). Its heavy mineral assemblage consists of cummingtonite and biotite with minor amounts of hornblende and orthopyroxene (Matsu'ura et al., 2002, 2003). We determined the Fe and Mg contents of the cummingtonite as 2.16–2.38 and 3.75–4.08, respectively (Fig. 4b). Representative major-element compositions are shown in Table 1.

Naruko–Nisaka tephra (N–N)

The Naruko–Nisaka tephra (N–N) was erupted from the Naruko caldera (Soda, 1989; Fig. 2). Its eruptive age is MIS 5.2–5.3 because it is stratigraphically above the On–Pm1 (MIS 5.3), Dks (MIS 5.3–5.2), and it is below the Aso-4 (MIS 5.2) (Soda, 1989). In this area, N–N is above Dks (locs. 2, 3, and 4) and below Aso-4 and the Yakeishi–Yamagata tephra (Yk–Y, 82 ka, described later) (loc. 2), and consists of distal fallout pumice and ash (Fig. 3). We first identified these distal deposits at locs. 2 and 3 as N–N tephra deposits on the basis of their glass-shard

https://doi.org/10.1016/j.yqres.2010.12.004 Published online by Cambridge University Press

chemistry (Table 2) and stratigraphic position relative to Aso-4, Dks, and On–Pm1. Although the reported heavy mineral assemblage of N–N consists of orthopyroxene and magnetite (Soda, 1989), trace amounts of hornblende and cummingtonite have been detected in N–N pyroclastic flow deposits (Matsu'ura et al., 2009). The N–N cummingtonite is divided into two groups on the basis of its chemical composition: the N–N 1 group (Fe, 2.26–2.39; Mg, 3.79–3.96) and the N–N 2 group (Fe, 3.02–3.11; Mg, 4.27–4.33) (Fig. 4c). Representative major-element compositions are shown in Table 1.

Cummingtonite-bearing tephras not expected at Kesennuma from previous isopach mapping

Adachi–Medeshima tephra (Ac–Md)

The Adachi–Medeshima tephra (Ac–Md) was erupted from the Adachi volcano in central NE Japan (Fig. 2; Kanisawa and Yoshida, 1989). Its eruptive age is older than MIS 5.2 because it is stratigraphically below Aso-4 (MIS5.2: Yagi and Soda, 1989; Aoki, 2008). The Ac–Md 0-cm isopach (Machida and Arai, 2003; Fig. 2) shows a distribution that does not include loc. 1. The only heavy mineral that has been identified in Ac–Md is cummingtonite (Kanisawa and Yoshida, 1989). We determined the Fe and Mg contents of the cummingtonite (sample 9A1) as 2.17–2.34 and 4.09–4.25, respectively (Fig. 4d). Representative major-element compositions are shown in Table 1.

Numazawa–Shibahara tephra (Nm–SB)

The Numazawa–Shibahara tephra (Nm–SB) was erupted from the Numazawa caldera in southern NE Japan (Fig. 2; Suzuki et al., 2004). Its eruptive age has been estimated to be 110 ka or MIS 5.4–5.3 as it is above the Numazawa–Tagashira tephra (Nm–TG, 135–125 ka or MIS 6–5.5; Suzuki, 1999), and it is below On–Pm1 (MIS5.3: Suzuki et al., 2004).

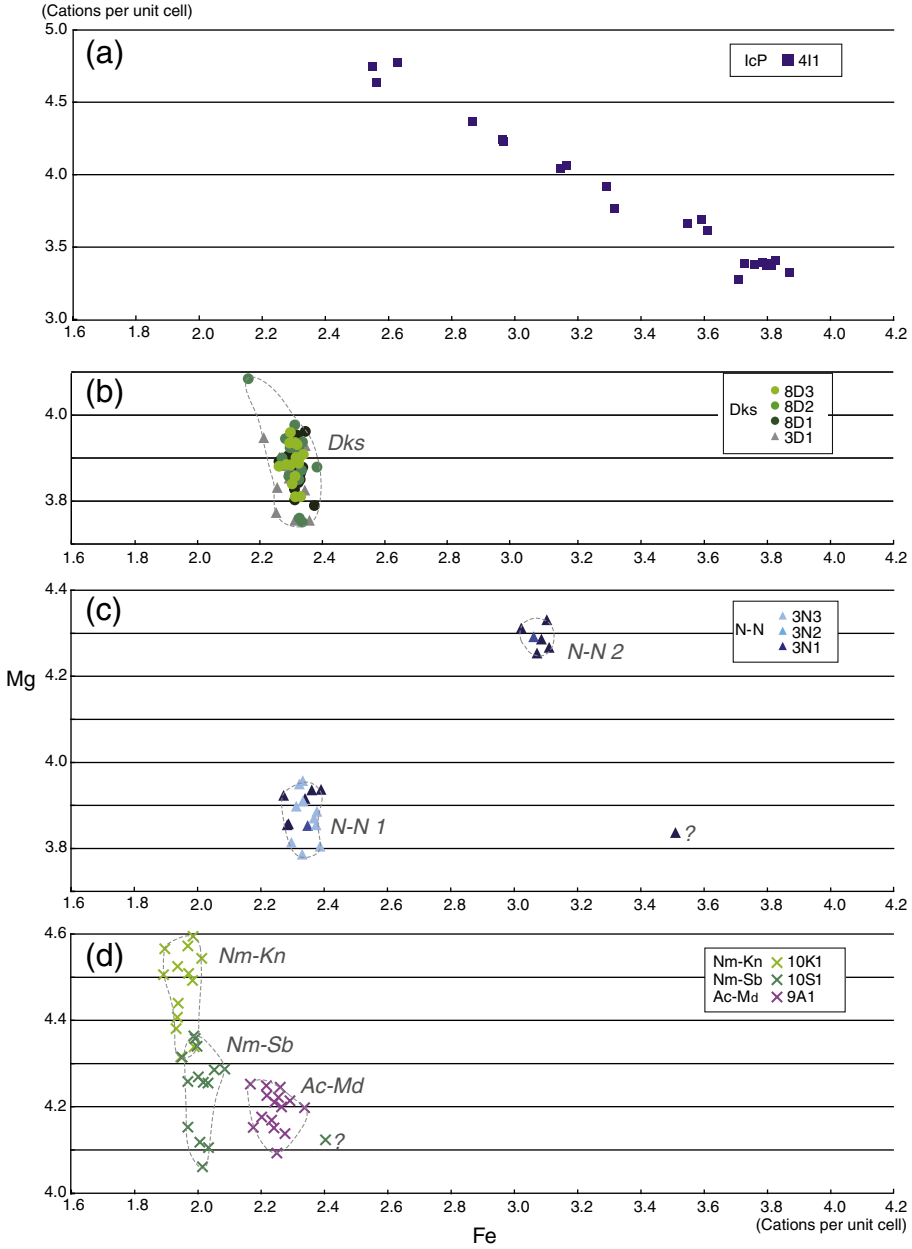

Figure 4. Fe–Mg compositions as cations per unit cell of cummingtonite in (a) IcP; (b) Dks; (c) N–N; (d) Ac–Md, Nm–KN, and Nm–SB; and in cryptotephras in loess deposits at (e) loc. 1; (f) loc. 2', and (g) loc. 7.

https://doi.org/10.1016/j.yqres.2010.12.004 Published online by Cambridge University Press

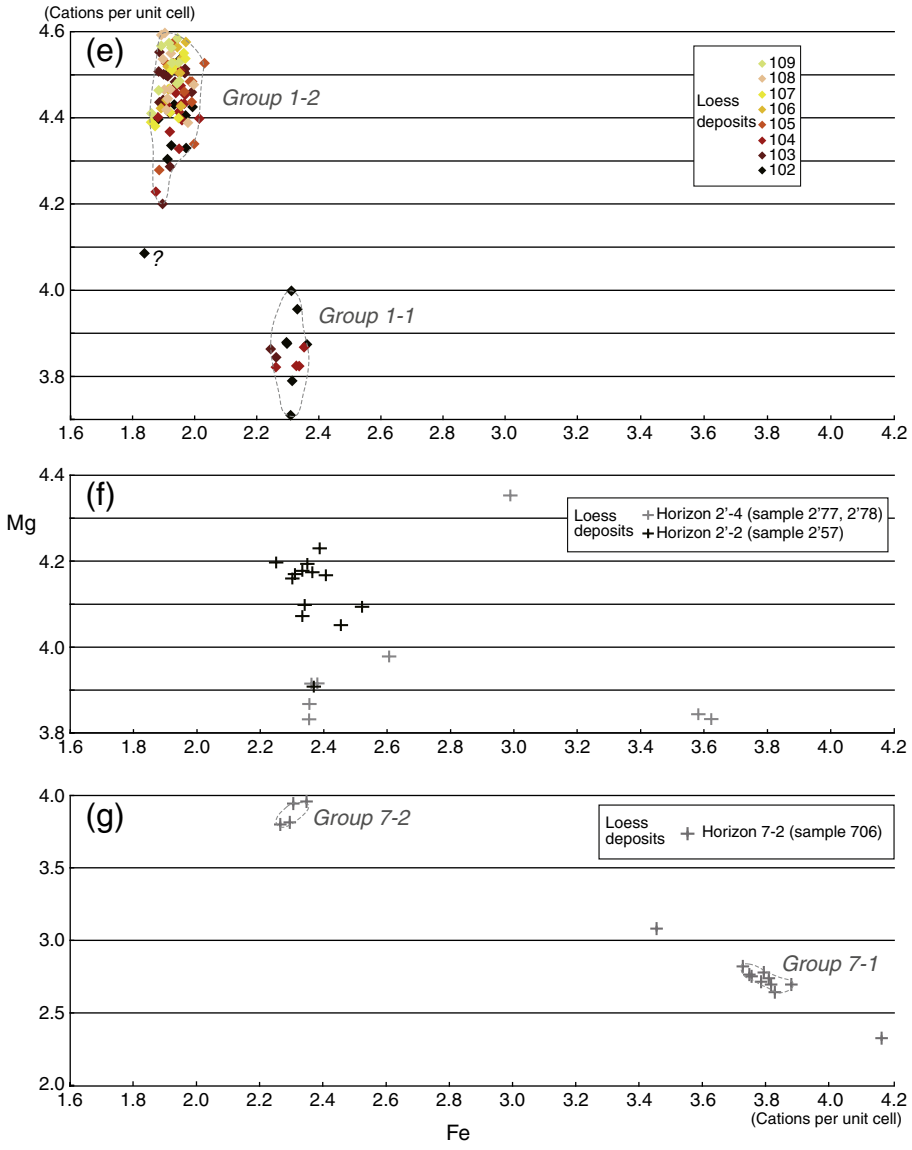

Figure 4 (*continued*).

Table 1
Representative chemical compositions of cummingtonite. Oxide composition of cummingtonite is shown as weight %. Numbers of cations are based on O = 23.

Sample	Dks (8D1)	N–N 1 (3N1)	N–N 2 (3N1)	Unknown (3N1)	Ac–Md	Nm–SB	Nm–KN	Group 1-1 (102)	Group 1-2 (107)
SiO_2	54.53	52.67	51.38	49.56	55.98	53.61	54.86	52.08	53.92
TiO_2	0.26	0.18	0.14	0.05	0.36	0.09	0.15	0.18	0.42
Al_2O_3	1.37	1.41	0.42	0.27	2.08	2.86	1.37	1.38	2.18
FeO	18.88	18.99	25.27	27.54	19.73	20.13	16.96	18.30	16.08
MnO	4.16	4.18	1.12	2.16	1.62	1.63	1.68	4.32	1.87
MgO	18.24	17.83	19.79	16.89	20.35	19.36	21.46	17.35	20.99
CaO	1.82	1.52	1.24	1.09	0.95	1.20	1.65	1.36	2.02
Na_2O	0.31	0.39	0.00	0.04	0.17	0.26	0.26	0.20	0.30
K_2O	0.00	0.00	0.02	0.00	0.03	0.00	0.00	0.01	0.01
Total (wt.%)	99.58	97.17	99.38	97.60	101.27	99.14	98.39	95.17	97.78
Si	7.81	7.76	7.54	7.55	7.78	7.66	7.79	7.81	7.70
Al	0.23	0.02	0.02	0.01	0.34	0.48	0.23	0.24	0.37
Ti	0.03	0.24	0.07	0.05	0.04	0.01	0.02	0.02	0.05
Fe	2.26	2.34	3.10	3.51	2.29	2.40	2.01	2.30	1.92
Mn	0.51	0.52	0.14	0.28	0.19	0.20	0.20	0.55	0.23
Mg	3.89	3.92	4.33	3.84	4.21	4.12	4.54	3.88	4.47
Ca	0.28	0.24	0.20	0.18	0.14	0.18	0.25	0.22	0.31
Na	0.09	0.11	0.00	0.01	0.05	0.07	0.07	0.06	0.08
K	0.00	0.00	0.00	0.00	0.01	0.00	0.00	0.00	0.00

https://doi.org/10.1016/j.yqres.2010.12.004 Published online by Cambridge University Press

Table 2
Chemical compositions of N–N glass shards determined by electron microprobe analysis of *n* glass shards. Means (±1 sigma) of normalized data are also given. Sample N–N data are from Matsu'ura et al. (2009).

Sample	3N1			3N2			3N3			N-N		
	Mean	Normalized mean	±1 σ	Mean	Normalized mean	±1 σ	Mean	Normalized mean	±1 σ	Mean	Normalized mean	±1 σ
SiO_2	74.66	78.50	(0.44)	74.58	79.06	(0.53)	74.64	78.97	(0.69)	74.78	78.79	(0.41)
TiO_2	0.21	0.22	(0.05)	0.17	0.18	(0.05)	0.18	0.19	(0.06)	0.16	0.17	(0.04)
$Al2O_3$	11.62	12.22	(0.27)	11.44	12.13	(0.18)	11.42	12.08	(0.40)	11.35	11.96	(0.31)
FeO[a]	1.36	1.42	(0.15)	1.25	1.33	(0.13)	1.17	1.25	(0.38)	1.32	1.39	(0.08)
MnO	0.09	0.09	(0.07)	0.07	0.07	(0.05)	0.09	0.09	(0.04)	0.05	0.05	(0.04)
MgO	0.16	0.17	(0.04)	0.09	0.10	(0.06)	0.12	0.12	(0.07)	0.14	0.15	(0.05)
CaO	1.32	1.38	(0.14)	1.19	1.26	(0.20)	1.12	1.19	(0.33)	1.29	1.36	(0.07)
Na_2O	4.04	4.25	(0.16)	3.74	3.96	(0.43)	3.84	4.06	(0.28)	4.08	4.30	(0.09)
K2O	1.66	1.75	(0.21)	1.81	1.92	(0.13)	1.93	2.04	(0.64)	1.74	1.83	(0.09)
Total	95.12	100.00		94.34	100.00		94.51	100.00		94.91	100.00	
n	12			6			11			15		

[a] Total iron denoted as FeO.

Nm–SB, which is above the Adatara–Dake tephra (Ad–Dk) and below the Adatara–N3 tephra (Ad–N3) (both erupted from the Adatara volcano; Fig. 2) at loc. 10, consists of fallout ash (Fig. 3). The Nm–SB 0-cm isopach is far from Kesennuma (Suzuki et al., 2004; Fig. 2). The heavy mineral assemblage of Nm–SB consists of hornblende, cummingtonite, and biotite, with minor amounts of orthopyroxene (Suzuki et al., 2004). We determined the Fe and Mg contents of the cummingtonite (sample 10 S1) as 1.95–2.09 and 4.06–4.36, respectively (Fig. 4d). Representative major-element compositions are shown in Table 1.

Numazawa–Kanayama tephra (Nm–KN)

The Numazawa–Kanayama tephra (Nm–KN) was erupted from the Numazawa caldera in southern NE Japan (Fig. 2; Suzuki et al., 2004). Nm–KN is between Aso-4 and the Daisen–Kurayoshi tephra (DKP) within the loess deposits (Suzuki and Soda, 1994). Its eruptive age was previously estimated to be 50–55 ka by assuming a constant accumulation rate of the loess between Aso-4 (MIS5.2, 86.8–87.3 ka; Aoki, 2008) and DKP (50–52 ka) (Suzuki and Soda, 1994). However, the estimated eruptive age of DKP has recently been revised to ≥55 ka (Machida and Arai, 2003), older than the previous estimation, so the eruptive age of Nm–KN can now be estimated as ca. 60 ka. Nm–KN, which is stratigraphically above Ad–N3 and below DKP and Adatara–N2 (Ad–N2) at loc. 10, consists of fallout ash (Fig. 3). Its 5-cm isopach is far from loc. 1 (Kesennuma) (Suzuki and Soda, 1994; Fig. 2), but its 0-cm isopach has not been identified. Its heavy mineral assemblage consists of hornblende, cummingtonite, and biotite (Suzuki and Soda, 1994). We determined the Fe and Mg contents of the cummingtonite (sample 10 K1) as 1.89–2.01 and 4.31–4.59, respectively (Fig. 4d). Representative major-element compositions are shown in Table 1.

Cummingtonite-free tephras identified at Kesennuma on the basis of isopach distribution patterns

Naruko–Yanagisawa tephra (N–Y)

The Naruko–Yanagisawa tephra (N–Y) was erupted from the Naruko caldera (Soda, 1989; Fig. 2). Its eruptive age is 50,900±2200 ^{14}C yr BP (NUTA-592; Nakai, 1988), 31.6–57.0 ka (thermoluminescence dating: Ichikawa, 1983; Ichikawa and Hiraga, 1988), and 40.3–63.4 ka (glass fission-track dating: Koshimizu, 1983). N–Y consists of fallout pumice and ash (loc. 5), surge deposits (loc. 6), and pyroclastic flow deposits (locs. 5 and 6) in ascending order (Fig. 3). Its heavy mineral assemblage consists of orthopyroxene and hornblende with minor amounts of magnetite, biotite, clinopyroxene, and olivine (Soda, 1989). Cummingtonite was not detected in any N–Y samples (5 N1, 5 N2, and 6 N1–6 N4) even by careful microscopic examination.

Yakeishi–Yamagata tephra (Yk–Y)

The Yakeishi–Yamagata tephra (Yk–Y) was erupted from the Yakeishi volcano (Okami and Yoshida, 1984; Fig. 2). Its eruptive age is 82±19 ka, determined by zircon fission-track dating (Watanabe et al., 2003). Yk–Y consists of fallout pumice at loc. 2 (Fig. 3). Its heavy mineral assemblage is reported to consist of orthopyroxene, clinopyroxene, and hornblende (Okami and Yoshida, 1984). A minor amount of biotite was found in Yk–Y at loc. 2 (sample 2Y1), but no cummingtonite was detected by careful microscopic examination.

Cummingtonite concentrations in the loess deposits and the cummingtonite geochemistry

Loess deposits at Kesennuma (loc. 1)

Samples of soil and loess deposits on the MIS 5.5 marine terrace surface at loc. 1 were obtained by rotary coring (Fig. 2). The stratigraphic column of the core at loc. 1 has been reported by Matsu'ura et al. (2009). The loess deposits at loc. 1 do not include any visible tephras but do contain concentrations of unweathered volcanic glass shards and minerals (crystals) (Fig. 5). Contiguous core samples 101 to 109 contain glass shards, orthopyroxene, and hornblende, and trace amounts of cummingtonite are also present. Tephras Dks, N–N, and N–Y were detected on the basis of the glass-shard major-element compositions and the refractive indices of orthopyroxene, hornblende, and cummingtonite (Matsu'ura et al., 2009: Fig. 5). Further, Matsu'ura et al. (2009) divided the cummingtonite (samples 101, 102, and 103 of this study) into two groups on the basis of its refractive indices. Here, we used only samples 102 to 109 for the chemical analysis of the cummingtonite because all cummingtonite grains in sample 101 (at the bottom of the loess deposits) had been already been picked out for measuring their refractive indices (Matsu'ura et al., 2009). We found that the cummingtonite could also be divided into two groups on the basis of its major-element chemistry: groups 1-1 and 1-2 (Fig. 4e). Group 1-1 is characterized by high Fe (2.27–2.39) and low Mg (3.79–4.00) contents and is found in samples from the base of the loess deposits (samples 1–2 to 1–4). Group 1-2 is characterized by low Fe (1.86–2.03) and high Mg (4.20–4.60) contents and is found mainly in samples from the upper part of the deposits. Thus, the group 1-1 cummingtonite is older than the group 1-2 cummingtonite. With respect to its Fe and Mg contents, group 1-1 is similar to the populations of Dks and N–N 1.

Loess deposits near Naruko volcano (loc. 7)

The soil and loess deposits on a fluvial terrace surface at loc. 7 were sampled by rotary boring (Fig. 2). The eolian sediments consist of loess and tephras Dks, N–Y, and H–O (Fig. 5). H–O is present as a clearly visible layer of fallout pumice, but the Dks or N–Y fallout ash layers are difficult to discern in the loess deposits and are best described as cryptotephras. Contiguous core samples 701 to 713 contained glass shards, orthopyroxene, and hornblende. Small amounts of cummingtonite were present in horizons 7-1 and 7-2, in the lower part of the loess deposits. In horizon 7-1, a clear cummingtonite concentration spike corresponds to the

https://doi.org/10.1016/j.yqres.2010.12.004 Published online by Cambridge University Press

stratigraphic position of Dks. Horizon 7-2 is probably an N–N cryptotephra because it lies between Dks and N–Y. No cummingtonite is present above horizon 7-2, which confirms that the distal N–Y deposit, like the deposits at locs. 5 and 6, does not include cummingtonite. The cummingtonite from horizon 7-2 (sample 706) can be divided into two groups, 7-1 and 7-2, on the basis of its composition (Fig. 4g). Group 7-1 is characterized by high Fe (3.73–3.88) and low Mg (2.64–2.82) contents, and group 7-2 by low Fe (2.27–2.35) and high Mg (3.80–3.96) contents. With respect to its Mg and Fe contents, group 7-2 is similar to the Dks and N–N 1 populations, but group 7-1 does not resemble any other tephra populations.

Loess deposits on the Isawa upland (loc. 2')

Mid and late Pleistocene loess and tephra sequences were observed on the Isawa upland at loc. 2', about 50 m southwest from loc. 2 (Fig. 2). The geological column at loc. 2' (Fig. 5) has been described previously (loc. 1 in Matsu'ura et al., 2008). The loess deposits include cummingtonite grains in four horizons: in ascending order, horizon 2'-1, between the Hinata 1 pumice (Hn1P) and the Hagimori white ash (HWA); horizons 2'-2 and 2'-3, between HWA and Yk–Y; and horizon 2'-4, above Yk–Y (Fig. 5). We correlated the cummingtonite in horizon 2'-3 with Dks and N–N because these ash layers occur in that horizon at loc. 2'. Cummingtonite is continuously present in horizons 2'-2 and 2'-3, but the chemistry of the cummingtonite in horizon 2'-2 (sample 2'57: Fe, 2.25–2.52; Mg, 3.91–4.23; Fig. 4f) is different from that of the Dks, N–N 1, and N–N 2 populations (Fig. 4b and c). The cummingtonite chemistry in horizon 2'-1 (samples 2'77 and 2'78: Fe, 2.36–3.63; Mg, 3.83–4.35; Fig. 4f) is also different from those of the Dks, N–N 1, and N–N 2 populations.

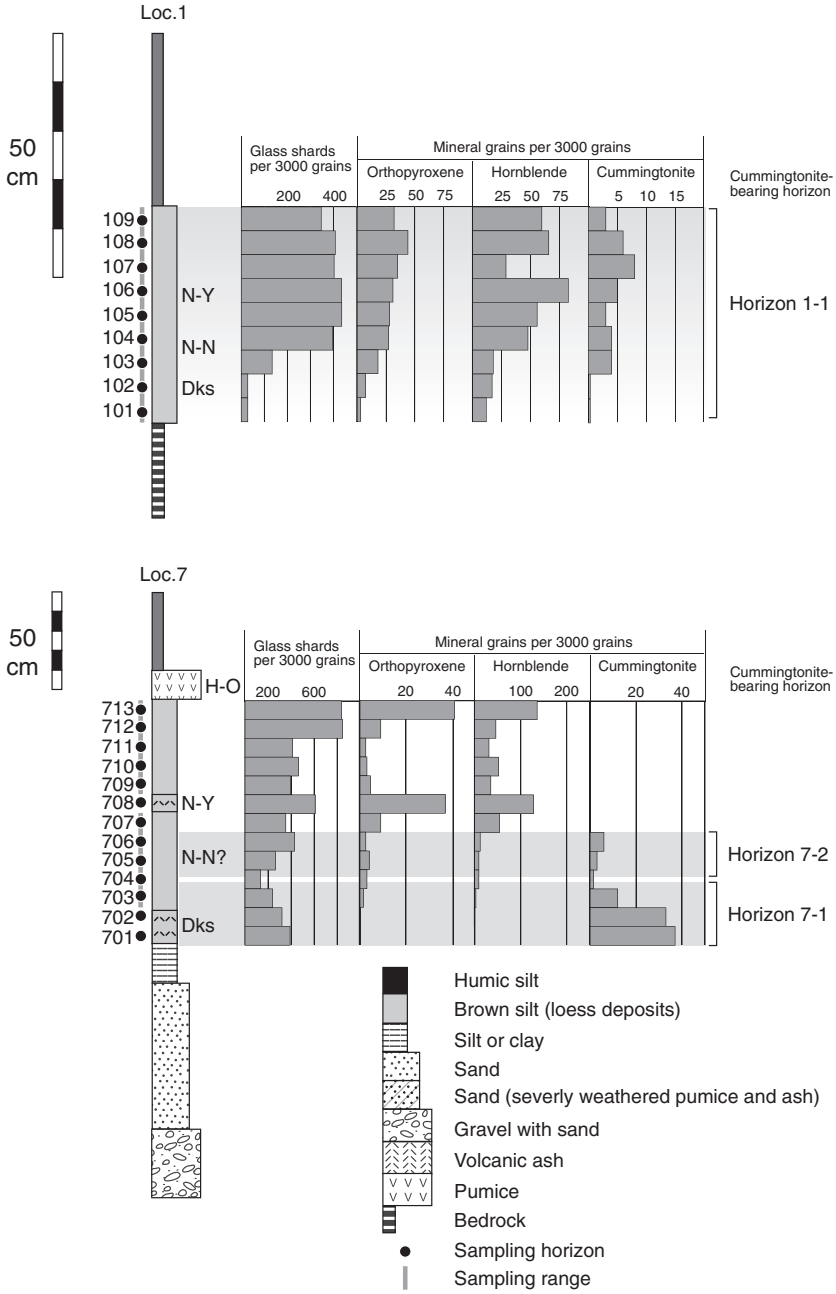

Figure 5. Geological columns showing the frequencies of glass shards and the ferromagnesian mineral assemblage of cryptotephras in the loess deposits at locs 1, 7, and 2'. Columns of locs. 1 and 7 are based on drill cores; loc. 2' is an outcrop.

https://doi.org/10.1016/j.yqres.2010.12.004 Published online by Cambridge University Press

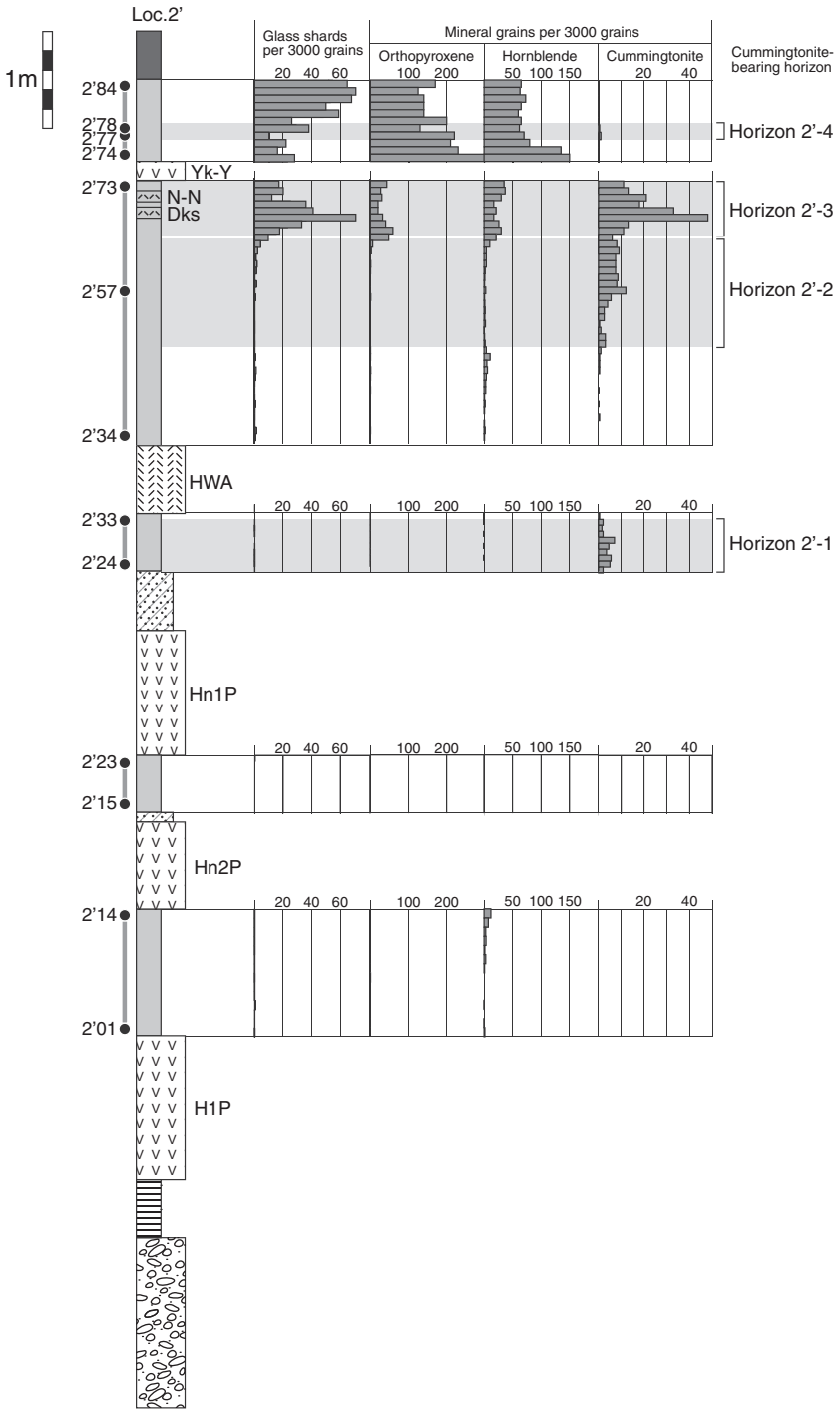

Figure 5 (*continued*).

Discussion

Cryptotephra correlation based on cummingtonite crystal concentrations and cummingtonite phase chemistry

The cummingtonite chemistry of the loess deposits at loc. 1 comprises two populations, groups 1-1 and 1-2 (Fig. 4e). The group 1-1 chemistry, in samples from the lower part of the loess deposits (samples 102 to 104), overlaps that of the Dks and N–N 1 populations (Fig. 4b and c). Therefore, the lower loess deposits include cummingtonite-bearing cryptotephras that can be correlated with Dks or N–N. The chemistry of group 1-2, mainly from the upper part of the loess deposits, does not overlap with that of the IcP, Dks, or N–N populations (Fig. 4a–c). Furthermore, group 1-2 cummingtonite does not originate from N–Y or Yk–Y because we detected no cummingtonite in N–Y or Yk–Y samples even by careful microscopic examination. Thus, the group 1-2 cummingtonite is best described as representing an unidentified tephra distributed in the Kesennuma area (Fig. 2). This cummingtonite was previously reported to be an unknown cryptotephra in the loess deposits with indeterminate stratigraphic position and age (Matsu'ura et al., 2009). By using our

https://doi.org/10.1016/j.yqres.2010.12.004 Published online by Cambridge University Press

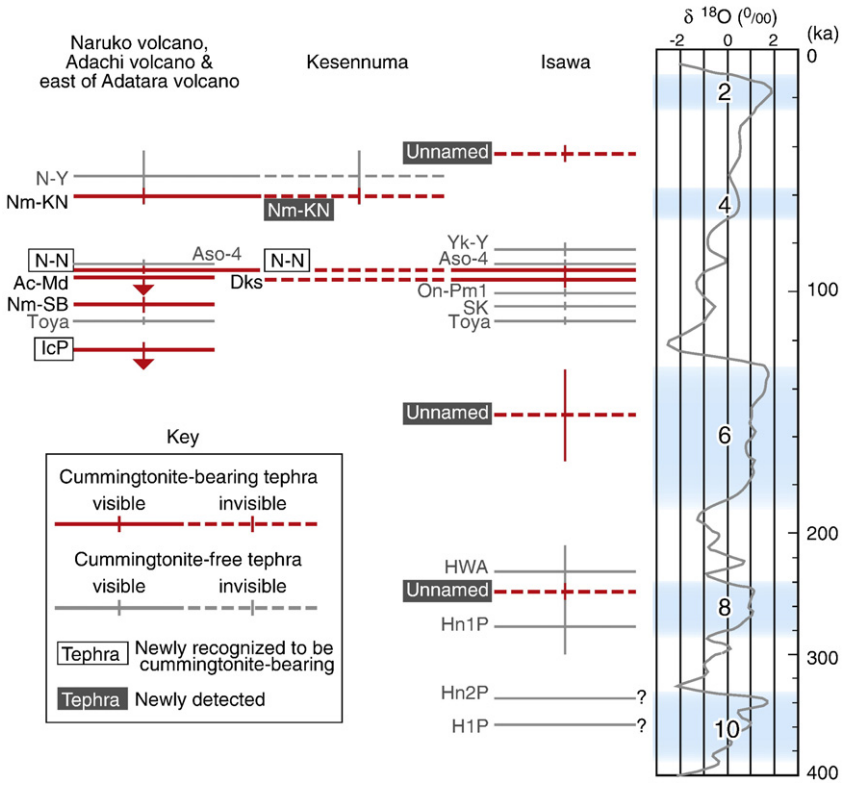

Figure 6. Late Quaternary tephra–cryptotephra correlations for central and southern NE Japan. Stratigraphic relationships among the tephras, terrace deposits, and the marine $^{18}\delta O$ curve (from Bassinot et al., 1994) are also shown. Blue shaded parts labeled with even numbers represent glacial periods. Downward arrows associated with Ac–Md and IcP indicate that their eruptive ages are minimum values.

cummingtonite-bearing cryptotephra method, we determined the stratigraphic position of this unidentified cummingtonite-bearing cryptotephra to be clearly above (younger than) Dks and N–N, but its relationship with N–Y and Yk–Y is unclear.

Even if the distribution of a named tephra does not include the Kesennuma area (Figs. 1 and 2), such a tephra might occur as a cryptotephra in the loess deposits at Kesennuma (loc. 1). We cannot, however, correlate this cryptotephra at loc. 1 with Ac–Md or Nm–SB, because their cummingtonite chemistries are different from that of the group 1-2 population (Fig. 4d and e). In contrast, Nm–KN, whose 5-cm isopach (Suzuki and Soda, 1994; Fig. 2) is far from Kesennuma, may occur as a cryptotephra at Kesennuma (loc. 1) because its cummingtonite chemistry overlaps with that of the group 1-2 population (Fig. 4d and e). Therefore, we attribute the group 1-2 cummingtonite at loc. 1 to a cummingtonite-bearing Nm–KN cryptotephra, previously unidentified in the loess deposits there.

Glass shards and hornblende of Nm–KN are also probably included in the loess deposits at loc. 1. At loc. 1, the glass shards and hornblende grains associated with Nm–KN cannot be easily discriminated from the large amounts of glass shards and hornblende from N–Y or other tephras. On the other hand, the small amount of cummingtonite in the loess deposits provides a powerful tool for detection of the cummingtonite-bearing Nm–KN cryptotephra in these loess deposits. The eruptive age of Nm–KN, ca. 60 ka, is consistent with the stratigraphic position of the group 1-2 cummingtonite concentration above Dks and N–N (MIS 5.2–5.3). Thus, Nm–KN was erupted from the Numazawa caldera and was carried far beyond the Adachi volcano all the way to Kesennuma (Fig. 2). Our cummingtonite-bearing cryptotephra detecting method has thus enabled us to improve our knowledge of the age and stratigraphy of the loess deposits at Kesennuma by showing that Dks, N–N, and Nm–KN cummingtonite-bearing cryptotephras are present in descending order (Fig. 6).

Other late Pleistocene cummingtonite-bearing cryptotephras were found at locs. 2' and 7. At loc. 2', a cummingtonite-bearing cryptotephra is present above Yk–Y, in horizon 2'-4 (Fig. 5). Because the chemistry of the cummingtonite in horizon 2'-4 does not overlap that of the Nm–KN population, that cummingtonite must be from an unidentified tephra (Fig. 6). At loc. 7, the cummingtonite in horizon 7-2 (sample 706) comprises groups 7-1 and 7-2 (Fig. 4g). We correlated group 7-2 with Dks or N–N on the basis of its cummingtonite chemistry, but we were not able to correlate group 7-1 with any cummingtonite-bearing tephra in central or southern NE Japan. Because loc. 7 is close to volcanoes of the inner arc, the group 7-1 cummingtonite may be from an unidentified cummingtonite-bearing cryptotephra derived from one of these volcanoes.

Detection and analysis of cummingtonite-bearing cryptotephras in mid Pleistocene loess deposits

It is generally difficult to detect cryptotephras of mid Pleistocene age in loess deposits because glass shards tend to be sparsely represented and easily dissolved by weathering, as noted earlier. Common minerals in tephras such as pyroxenes and hornblende are resistant to weathering, but their concentrations, refractive indices, and chemistry are not distinctive among tephras in central NE Japan (Machida and Arai, 2003). Cummingtonite, however, might be useful as an indicator of mid Pleistocene cryptotephras. We identified four cummingtonite-bearing horizons in the mid and late Pleistocene loess deposits at loc. 2' (Fig. 5). We correlated horizon 2'-3 with Dks and N–N (MIS 5.2–5.3) on the basis of its stratigraphic position in relation to that of Dks and N–N. We therefore attribute horizons 2'-1 and 2'-2, which are below Dks, to mid Pleistocene cummingtonite-bearing cryptotephras. Cummingtonite grains in horizons 2'-1 and 2'-2 did not originate from the known mid Pleistocene tephras H1P, Hn2P, Hn1P, or HWA because these tephras do not contain

https://doi.org/10.1016/j.yqres.2010.12.004 Published online by Cambridge University Press

cummingtonite (Matsu'ura et al., 2008). Moreover, horizons 2'-1 and 2'-2 do not show any evidence of cryptotephras such as concentrations of glass shards or of any minerals (Fig. 5).

The age of horizon 2'-1 is about 250 ka, because horizon 2'-1 is between HWA (210–250 ka) and Hn1P (250–300 ka) (Matsu'ura et al., 2008; Fig. 6). The age of horizon 2'-2 must be 100–200 ka because horizon 2'-2 is above HWA and below Dks. In distal areas, where Hn1P and HWA are present in the loess only as cryptotephras, these cummingtonite-bearing cryptotephra deposits will be useful for establishing a new tephrostratigraphy, because the refractive indices and mineral chemistries of the mid Pleistocene Hn1P and HWA tephras are not distinctive.

Conclusions

We detected late Pleistocene cummingtonite-bearing cryptotephras in loess deposits and correlated them with reported tephras in NE Japan on the basis of the cummingtonite chemistry, especially Fe and Mg concentrations, and stratigraphic considerations. This is the first time cryptotephras have been correlated using crystal rather than glass-shard compositions. We also detected cummingtonite-bearing cryptotephras for the first time in mid Pleistocene loess sediments. Our main conclusions are:

(1) We detected cummingtonite for the first time in the Ichihasama tephra (IcP) and confirmed that cummingtonite-bearing tephras, namely, the IcP tephra and the Dokusawa (Dks) and Naruko–Nisaka (N–N) tephras, are present as cryptotephras in late Pleistocene eolian sediments in central NE Japan.
(2) The cummingtonite chemistries of the IcP, Dks, and N–N tephras differ from one another and are diagnostic. Therefore, geochemical analysis of cummingtonite grains provides a powerful tool for detecting distal occurrences of these tephras as cryptotephras.
(3) One cummingtonite-bearing cryptotephra in the late Pleistocene loess deposits at Kesennuma (Pacific coast) does not correlate with any cummingtonite-bearing tephras known to occur in central NE Japan, but it can be correlated with Numazawa–Kanayama tephra (Nm–KN), erupted from the Numazawa caldera, southern NE Japan, on the basis of its cummingtonite chemistry.
(4) Use of our new cummingtonite-bearing cryptotephra detecting method has improved our knowledge of the stratigraphy of the loess deposits at Kesennuma by showing that the Dks, N–N, and Nm–KN cummingtonite-bearing cryptotephras, in descending order, are present in the loess deposits.
(5) Three unnamed horizons containing cummingtonite concentrations were detected for the first time in mid and late Pleistocene loess deposits on the Isawa upland. These horizons occur above Dks (MIS 5.2–5.3), between Dks and Hagimori white ash (HWA: 210–250 ka), and between HWA and Hinata 1 pumice (Hn1P: 250–300 ka). Such cummingtonite-bearing cryptotephras will be useful for establishing the chronology of mid and late Pleistocene sediments in central NE Japan.

Acknowledgments

We thank S. Kanisawa (Tohoku University), J. Itoh, K. Ikehara (Geological Survey of Japan), and T. Yoshiki (Iwate Prefectural University) for their constructive comments, and T. Suzuki (Tokyo Metropolitan University) and T. Soda (Tephro-archeological Research Institute) for explaining the stratigraphy of loc. 10 at the 8th COT-J field workshop. We are appreciative of the editors (A. Gillespie and A. Singhvi) and reviewers for their helpful comments. We are also grateful to D. Lowe (University of Waikato) for his helpful advice. Some figures were prepared with Generic Mapping Tool version 4.2.0 (Wessel and Smith, 1998). This research project was conducted under a research contract with the Nuclear and Industrial Safety Agency of Japan (NISA).

References

Aoki, K., 2008. Revised age and distribution of ca. 87 ka Aso-4 tephra based on new evidence from the northwest Pacific Ocean. Quaternary International 178, 100–118.
Aoki, K., Arai, F., 2000. Late Quaternary tephrostratigraphy of marine core KH-94-3, LM-8 Sanriku, Japan. The Quaternary Research (Japan) 39, 107–120 (in Japanese with English abstract).
Bassinot, F.C., Labeyrie, L.D., Vincent, E., Quidelleur, X., Shackleton, N.J., Lancelot, Y., 1994. The astronomical theory of climate and the age of the Brunhes–Matuyama magnetic reversal. Earth and Planetary Science Letters 126, 91–108.
Davies, S.M., Wastegård, S., Abbott, P.M., Barbante, C., Bigler, M., Johnsen, S.J., Rasmussen, T.L., Steffensen, J.P., Svensson, A., 2010. Tracing volcanic events in the NGRIP ice-core and synchronising North Atlantic marine records during the last glacial period. Earth and Planetary Science Letters 294, 69–79.
de Fontaine, C.S., Kaufman, D.S., Anderson, R.S., Werner, A., Waythomas, C.F., Brown, T.A., 2007. Late Quaternary distal tephra-fall deposits in lacustrine sediments, Kenai Peninsula, Alaska. Quaternary Research 68, 64–78.
Gehrels, M.J., Lowe, D.J., Hazell, Z.J., Newnham, R.M., 2006. A continuous 5300-yr Holocene cryptotephrostratigraphic record from northern New Zealand and implications for tephrochronology and volcanic hazard assessment. The Holocene 16, 173–187.
Gehrels, M.J., Newnham, R.M., Lowe, D.J., Wynne, S., Hazell, Z.J., Caseldine, C., 2008. Towards rapid assay of cryptotephra in peat cores: review and evaluation of various methods. Quaternary International 178, 68–84.
Geschwind, C.-H., Rutherford, M.J., 1992. Cummingtonite and the evolution of the Mount St. Helens (Washington) magma systems: an experimental study. Geology 20, 1011–1014.
Ichikawa, Y., 1983. In: Sekki bunka danwa-kai (Ed.), Thermoluminescence Ages of the Zazaragi Site and Its Environment: Zazaragi site, Tagajo-shi, pp. 95–96 (in Japanese).
Ichikawa, Y., Hiraga, S., 1988. Thermoluminescence Ages of Some Paleolithic Sites in Miyagi Prefecture: Program and abstracts of the Japan Association for Quaternary Research, 18, pp. 46–47 (in Japanese).
Kanisawa, S., Yoshida, T., 1989. Genesis of the extremely low-K tonalites from the island arc volcanism: lithic fragments in the Adachi–Medeshima pumice deposits, northeast Japan. Bulletin of Volcanology 51, 346–354.
Koshimizu, T., 1983. In: Sekki bunka danwa-kai (Ed.), Fission-track Ages of the Zazaragi Site and Its Environment: Zazaragi site, Tagajo-shi, pp. 97–99 (in Japanese).
Lim, C., Ikehara, K., Toyoda, K., 2008. Cryptotephra detection using high-resolution trace-element analysis of Holocene marine sediments, southwest Japan. Geochimica et Cosmochimica Acta 7, 5022–5036.
Lowe, D.J., 1988. Late Quaternary volcanism in New Zealand: towards an integrated record using distal airfall tephras in lakes and bogs. Journal of Quaternary Science 3, 111–120.
Lowe, D.J., 2008. Globalisation of tephrochronology — new views from Australasia. Progress in Physical Geography 32, 311–335.
Lowe, J.J., Blockley, S.P.E., Trincardi, F., Asioli, A., Cattaneo, A., Matthews, I.P., Pollard, A.M., Wulf, S., 2007. Age modelling of late Quaternary marine sequences in the Adriatic: towards improved precision and accuracy using volcanic event stratigraphy. Continental Shelf Research 27, 560–582.
Lowe, D.J., Hunt, J.B., 2001. A summary of terminology used in tephra-related studies. Les Dossiers de l'Archaeo-Logis 1, 17–22.
Lowe, D.J., Shane, P.A.R., Alloway, B.V., Newnham, R.M., 2008. Fingerprints and age models for widespread New Zealand tephra marker beds erupted since 30, 000 years ago: a framework for NZ-INTIMATE. Quaternary Science Reviews 27, 95–126.
Machida, H., Arai, F., 2003. Atlas of Tephra in and Around Japan. University of Tokyo Press, Tokyo. 336 pp., (in Japanese with English abstract).
Matsu'ura, T., Furusawa, A., Saomoto, H., 2008. Late Quaternary uplift rate of the northeastern Japan arc inferred from fluvial terraces. Geomorphology 95, 384–397.
Matsu'ura, T., Furusawa, A., Saomoto, H., 2009. Long-term and short-term vertical velocity profiles across the forearc in the NE Japan subduction zone. Quaternary Research 71, 227–238.
Matsu'ura, T., Nitta, E., Kanisawa, S., Nakashima, K., 2002. Dokusawa tephra erupted at approximately 100 ka and its eruptive process in the central part of northeast Japan. Bulletin of Volcanological Society of Japan 47, 711–725 (in Japanese with English abstract).
Matsu'ura, T., Nitta, E., Kanisawa, S., Nakashima, K., 2003. Correlation of Dokusawa and Kitahara Tephras in the Central Part of Northeast Japan — EPMA Analyses of Heavy Minerals: Science Report of Tohoku University 7th Series (Geography), 52, pp. 29–44.
Miyagi, I., 2004. On the eruption age of the Hijiori caldera, based on more accurate and reliable radiocarbon data. Bulletin of Volcanological Society of Japan 49, 201–205.
Mullineaux, D.R., 1986. Summary of pre-1980 tephra-fall deposits erupted from Mount St. Helens Washington State, USA. Bulletin of Volcanology 45, 17–26.

https://doi.org/10.1016/j.yqres.2010.12.004 Published online by Cambridge University Press

Nakai, N., 1988. In: Tohoku rekishi shiryo-kan, Sekki bunka danwa-kai (Eds.), Report on ^{14}C Dating of Babadan-A Site: Tohoku rekishi shiryo-kan shiryo-shu no.39, Tagajo-shi, p. 52 (in Japanese).
Okami, K., Yoshida, M., 1984. Tephrochronology of the Isawa Fan Area, Middle Course of the Kitakami River: Report on Technology of Iwate University, 137, pp. 69–81 (in Japanese with English abstract).
Payne, R., Blackford, J., van der Plicht, J., 2008. Using cryptotephras to extend regional tephrochronologies: an example from southeast Alaska and implications for hazard assessment. Quaternary Research 69, 42–55.
Shane, P., Frogatt, P., Smith, T., Gregory, M., 1998. Multiple source for sea-rafted Loisels pumices, New Zealand. Quaternary Research 49, 271–279.
Shane, P.A.L., Smith, V., Nairn, I.A., 2003. Biotite composition as a tool for the identification of Quaternary tephra beds. Quaternary Research 59, 262–270.
Smith, D.R., Leeman, W.P., 1982. Mineralogy and phase chemistry of Mount St. Helens tephra sets W and Y as keys to their identification. Quaternary Research 17, 211–227.
Smith, V.C., Shane, P., Nairn, I.A., 2005. Trends in rhyolite geochemistry, mineralogy, and magma storage during the last 50 kyr at Okataine and Taupo volcanic centres, Taupo Volcanic Zone, New Zealand. Journal of Volcanology and Geothermal Research 148, 372–406.
Smith, V.C., Shane, P.A.R., Nairn, I.A., Williams, C.M., 2006. Geochemistry and magmatic properties of eruption episodes from Haroharo linear vent zone, Okataine Volcanic Centre, New Zealand, during the last 10 kyr. Bulletin of Volcanology 69, 57–88.
Soda, T., 1989. Tephrochronological study of the layers including the early Paleolithic artifacts in the northern part of Sendai plain. The Quaternary Research (Japan) 28, 269–282 (in Japanese with English abstract).
Suzuki, T., 1999. Transgression and regression of MIS 5.5 and its related tephras recognized at the Tsukabara coast on Pacific Ocean, northeast Japan. Journal of Geography 108, 216–230.
Suzuki, T., 2001. Iizuna–Kamitaru tephra group erupted from the Iizuna volcano of Myoko volcano group in the transition from marine isotope stage 6 to 5, and its significance for the chronological study of central Japan. The Quaternary Research 40, 29–41 (in Japanese with English abstract).
Suzuki, T., 2008. Analysis of titanomagnetite within weathered middle Pleistocene KMT tephra and its application for fluvial terrace chronology, Kanto Plain, central Japan. Quaternary International 178, 119–127.
Suzuki, T., Fujiwara, O., Dangara, T., 2004. Stratigraphy and chronology of middle Pleistocene tephras in and around Aizu area, northwest Japan. Journal of Geography 113, 38–61 (in Japanese with English abstract).
Suzuki, T., Soda, T., 1994. Numazawa–Kanayama tephra erupted from Numazawa volcano at 50–55 ka in the southern part of the northwest Japan arc. The Quaternary Research (Japan) 33, 233–242 (in Japanese with English abstract).
Wagner, B., Sulpizio, R., Zanchetta, G., Wulf, S., Wessels, M., Daut, G., Nowaczyk, N., 2008. The last 40 ka tephrostratigraphic record of Lake Ohrid, Albania and Macedonia: a very distal archive for ash dispersal from Italian volcanoes. Journal of Volcanology and Geothermal Research 177, 71–80.
Wastegård, S., Davies, S.M., 2009. An overview of distal tephrochronology in northern Europe during the last 1000 years. Journal of Quaternary Science 24, 500–512.
Watanabe, M., Danhara, T., Fujiwara, O., 2003. Fission Track Ages of Quaternary Tephras and Chronology of Fluvial Terrace Surfaces in Southern Part of the Kitakami Lowland, Northeast Japan: Proceedings of the General Meeting of the Association of Japanese Geographers, 63, p. 111 (in Japanese).
Wessel, P., Smith, W.H.F., 1998. New, Improved Version of the Generic Mapping Tools Released: EOS Trans. AGU, 79, p. 579.
Wulf, S., Kraml, M., Keller, J., 2008. Towards a detailed distal tephrostratigraphy in the central Mediterranean: the last 20,000 yrs record of Lago Grande di Monticchio. Journal of Volcanology and Geothermal Research 177, 118–132.
Yagi, H., Soda, T., 1989. A stratigraphical study on the late Pleistocene widespread tephras occurring in central and northern part of Miyagi Prefecture. Journal of Geography 98, 39–53 (in Japanese with English abstract).

https://doi.org/10.1016/j.yqres.2010.12.004 Published online by Cambridge University Press